Limits on uranium and thorium bulk content in Gerda Phase I detectors

Baudis, Laura ; Kish, Alexander ; Mingazheva, Rizalina ; et al

Abstract: Internal contaminations of ^{238}U, ^{235}U and ^{232}Th in the bulk of high purity germanium detectors are potential backgrounds for experiments searching for neutrinoless double beta decay of ^{76}Ge. The data from Gerda Phase I have been analyzed for alpha events from the decay chain of these contaminations by looking for full decay chains and for time correlations between successive decays in the same detector. No candidate events for a full chain have been found. Upper limits on the activities in the range of a few nBq/kg for ^{226}Ra, ^{227}Ac and ^{228}Th, the long-lived daughter nuclides of ^{238}U, ^{235}U and ^{232}Th, respectively, have been derived. With these upper limits a background index in the energy region of interest from ^{226}Ra and ^{228}Th contamination is estimated which satisfies the prerequisites of a future ton scale germanium double beta decay experiment.

DOI: https://doi.org/10.1016/j.astropartphys.2017.03.003

Posted at the Zurich Open Repository and Archive, University of Zurich
ZORA URL: https://doi.org/10.5167/uzh-148793
Journal Article
Published Version

Originally published at:
Baudis, Laura; Kish, Alexander; Mingazheva, Rizalina; et al (2017). Limits on uranium and thorium bulk content in Gerda Phase I detectors. Astroparticle Physics, 91:15-21.
DOI: https://doi.org/10.1016/j.astropartphys.2017.03.003

Astroparticle Physics 91 (2017) 15–21

Contents lists available at ScienceDirect

Astroparticle Physics

journal homepage: www.elsevier.com/locate/astropartphys

Limits on uranium and thorium bulk content in GERDA Phase I detectors

GERDA collaboration, M. Agostini[a], M. Allardt[d], A.M. Bakalyarov[m], M. Balata[a], I. Barabanov[k], L. Baudis[s], C. Bauer[g], N. Becerici-Schmidt[n], E. Bellotti[h,i], S. Belogurov[l,k], S.T. Belyaev[m], G. Benato[s], A. Bettini[p,q], L. Bezrukov[k], T. Bode[o], D. Borowicz[c,e], V. Brudanin[e], R. Brugnera[p,q], A. Caldwell[n], C. Cattadori[i], A. Chernogorov[l], V. D'Andrea[a], E.V. Demidova[l], A. di Vacri[a], A. Domula[d], E. Doroshkevich[k], V. Egorov[e], R. Falkenstein[r], O. Fedorova[k], K. Freund[r], N. Frodyma[c], A. Gangapshev[k,g], A. Garfagnini[p,q], P. Grabmayr[r], V. Gurentsov[k], K. Gusev[e,m,o], J. Hakemüller[g], A. Hegai[r], M. Heisel[g], S. Hemmer[p,q], W. Hofmann[g], M. Hult[f], L.V. Inzhechik[k,t], J. Janicskó Csáthy[o], J. Jochum[r], M. Junker[a], V. Kazalov[k], T. Kihm[g], I.V. Kirpichnikov[l], A. Kirsch[g], A. Kish[s], A. Klimenko[g,e,u], R. Kneißl[o], K.T. Knöpfle[g], O. Kochetov[e], V.N. Kornoukhov[l,k], V.V. Kuzminov[k], M. Laubenstein[a], A. Lazzaro[o], V.I. Lebedev[m], B. Lehnert[d], H.Y. Liao[n], M. Lindner[g], I. Lippi[q], A. Lubashevskiy[g,e], B. Lubsandorzhiev[k], G. Lutter[f], C. Macolino[a,v], B. Majorovits[n], W. Maneschg[g], E. Medinaceli[p,q], R. Mingazheva[s], M. Misiaszek[c], P. Moseev[k], I. Nemchenok[e], D. Palioselitis[n], K. Panas[c], L. Pandola[b], K. Pelczar[c], A. Pullia[j], S. Riboldi[j], N. Rumyantseva[e], C. Sada[p,q], F. Salamida[i], M. Salathe[g], C. Schmitt[r], B. Schneider[d], S. Schönert[o], J. Schreiner[g], A.-K. Schütz[r], O. Schulz[n], B. Schwingenheuer[g], O. Selivanenko[k], E. Shevchik[e], M. Shirchenko[e], H. Simgen[g], A. Smolnikov[g,e], L. Stanco[q], M. Stepaniuk[g], L. Vanhoefer[n], A.A. Vasenko[l], A. Veresnikova[k], K. von Sturm[p,q], V. Wagner[g], M. Walter[s], A. Wegmann[g], T. Wester[d], C. Wiesinger[o], M. Wojcik[c], E. Yanovich[k], I. Zhitnikov[e], S.V. Zhukov[m], D. Zinatulina[e], K. Zuber[d], G. Zuzel[c]

[a] INFN Laboratori Nazionali del Gran Sasso, LNGS, and Gran Sasso Science Institute, GSSI, Assergi, Italy
[b] INFN Laboratori Nazionali del Sud, Catania, Italy
[c] Institute of Physics, Jagiellonian University, Cracow, Poland
[d] Institut für Kern- und Teilchenphysik, Technische Universität Dresden, Dresden, Germany
[e] Joint Institute for Nuclear Research, Dubna, Russia
[f] European Commission, JRC-Geel, Geel, Belgium
[g] Max-Planck-Institut für Kernphysik, Heidelberg, Germany
[h] Dipartimento di Fisica, Università Milano Bicocca, Milan, Italy
[i] INFN Milano Bicocca, Milan, Italy
[j] Dipartimento di Fisica, Università degli Studi di Milano e INFN Milano, Milan, Italy
[k] Institute for Nuclear Research of the Russian Academy of Sciences, Moscow, Russia
[l] Institute for Theoretical and Experimental Physics, Moscow, Russia
[m] National Research Centre "Kurchatov Institute", Moscow, Russia
[n] Max-Planck-Institut für Physik, Munich, Germany
[o] Physik Department and Excellence Cluster Universe, Technische Universität München, Munich, Germany
[p] Dipartimento di Fisica e Astronomia dell'Università di Padova, Padova, Italy
[q] INFN Padova, Padova, Italy
[r] Physikalisches Institut, Eberhard-Karls Universität Tübingen, Germany
[s] Physik Institut der Universität Zürich, Zürich, Switzerland
[t] Moscow Inst. of Physics and Technology, Moscow, Russia
[u] Int. Univ. for Nature, Society and Man "Dubna", Dubna, Russia
[v] LAL, Université Paris-Saclay, Orsay, France

E-mail address: gerda-eb@mpi-hd.mpg.de (GERDA Editorial Board).

http://dx.doi.org/10.1016/j.astropartphys.2017.03.003

ARTICLE INFO

Article history:
Received 18 November 2016
Revised 3 March 2017
Accepted 6 March 2017
Available online 7 March 2017

Keywords:
Germanium detectors
Double beta decay
Radiopurity
Uranium and thorium bulk content

ABSTRACT

Internal contaminations of ^{238}U, ^{235}U and ^{232}Th in the bulk of high purity germanium detectors are potential backgrounds for experiments searching for neutrinoless double beta decay of ^{76}Ge. The data from GERDA Phase I have been analyzed for alpha events from the decay chain of these contaminations by looking for full decay chains and for time correlations between successive decays in the same detector. No candidate events for a full chain have been found. Upper limits on the activities in the range of a few nBq/kg for ^{226}Ra, ^{227}Ac and ^{228}Th, the long-lived daughter nuclides of ^{238}U, ^{235}U and ^{232}Th, respectively, have been derived. With these upper limits a background index in the energy region of interest from ^{226}Ra and ^{228}Th contamination is estimated which satisfies the prerequisites of a future ton scale germanium double beta decay experiment.

1. Introduction

The unknown nature and the mass of the neutrino are among the biggest unsolved mysteries of modern particle physics. Observation of neutrinoless double beta ($0\nu\beta\beta$) decay could shed light onto these questions. The experimental search for neutrinoless $0\nu\beta\beta$ decay requires ultra sensitive detectors with a very low background rate like High Purity Germanium (HPGe) detectors. The GERDA experiment [1] has set the strongest lower bound for the half-life of $0\nu\beta\beta$ decay of ^{76}Ge [2,3]. Further generations of experiments with larger target masses have started or are in the planning stage [4].

In order to improve the sensitivity of HPGe detector based experiments, an increase of detector mass in combination with a further reduction of the radioactive background is necessary. In the next generation of experiments the detector mass could amount to about a ton of detector material while a background rate below ≈0.1 cts/(RoI· ton· yr) in the energy region of interest (RoI) will be necessary. This value is more than one order of magnitude lower than the level presently reached in GERDA Phase II [3]. In order to achieve such a low background level, it is necessary to investigate and eventually reduce all possible background components.

An important background contribution to all rare event searches is the natural radioactivity from isotopes of the ^{238}U, ^{235}U and ^{232}Th decay chains. Fig. 1 depicts the relevant and accessible part of the chains. Background in the RoI can among others be induced by several γ lines originating from the decays of ^{214}Bi and ^{208}Tl that are above the Q-value of $0\nu\beta\beta$ decay in ^{76}Ge, with $Q_{\beta\beta}$ = 2039 keV. The most prominent one in general is the 2614.5 keV line in ^{208}Pb following the ^{208}Tl β decay. These long-lived uranium and thorium isotopes are omnipresent in the earth's crust [5] and are to be expected in any natural material and surrounding. The purification process of germanium during production of HPGe crystals efficiently removes uranium and thorium. However, further processing steps in detector production and setup follow until the final deployment within the experiment. This might bring back some fraction of radioactivity, mostly on the surface. A tiny contamination of the bulk HPGe with these elements can deteriorate the sensitivity of HPGe experiments considerably. Simulations suggest that contaminations of ≈0.1 μBq/kg for ^{238}U and ^{232}Th account for an expected background rate of 1 cts/(RoI· ton· yr) and 0.2 cts/(RoI· ton· yr), respectively [6, and refs. therein] when a RoI of 4 keV around $Q_{\beta\beta}$ is assumed. Thus, for future ton-scale experiments the bulk contamination of HPGe can be a potential background source. This implies that the purity of HPGe has to be controlled to a level lower than 10 nBq/kg.

In this paper limits for the bulk contamination of HPGe detectors by isotopes of the decay chains ^{238}U, ^{235}U and ^{232}Th are given that are obtained from GERDA Phase I data. The spectrum of every detector was searched for a sequence of α decays occuring in the decay chains. In most cases at least one of the decays was missing. If candidates for all α decays exist the compartibility of the time distribution of the events with the expectation from the half lives is checked. The limits derived from GERDA Phase I data show for the first time that the bulk contamination of HPGe can be controlled to a level of a few nBq/kg for the isotopes ^{228}Th, ^{227}Ac and ^{226}Ra resulting from primordial ^{238}U, ^{235}U and ^{232}Th. This demonstrates that bulk contamination of HPGe with these isotopes is unlikely to limit a future ton-scale HPGe experiment for the search of $0\nu\beta\beta$ decay.

2. Experiment and data sets

The GERDA experiment consists of an array of germanium detectors submerged into a cryostat filled with liquid argon (LAr). The cryostat has a diameter of 4 m and is placed inside a water tank with a diameter of 10 m. In Phase I of the experiment, eight refurbished semi-coaxial HPGe detectors from the Heidelberg-Moscow [7] and IGEX [8] experiments made from germanium isotopically enriched in ^{76}Ge were deployed together with other semi-coaxial detectors with natural abundance [9]. Some detectors had been replaced by five enriched Broad Energy Germanium (BEGe) detectors [10]. Details of the GERDA experimental setup can be found in Ref. [1].

For the current analysis, all data recorded in the period between December 2, 2011 and September 5, 2013 inclusive those of the natural detectors were used which expands slightly the data set of Ref. [2] to 26.14 kg· yr. For the calibration of the energy scale GERDA uses ^{228}Th sources. Since the expected energy deposition of an internal α background is above the highest energetic calibration peak at 2.6 MeV, data from calibration runs were also used in the analysis. While the increase of exposure is not significant (< 2%), this extends the continuity of data taking which in turn improves the detection efficiency of the decay sequences (see Section 4). The longest live time for a subset of detectors corresponds to 543.8 days (see Table 1). Unphysical events due to electromagnetic noise or discharges are identified and rejected by a set of quality cuts. These cuts take into account parameters of the charge pulse, e.g. rise time and baseline fluctuations, and are described in Ref. [11]. Pile-up events, in which two distinct pulses are recorded during the digitization time window of 80 μs, are also discarded [12]. Events in coincidence with a muon trigger are rejected. The individual live times and masses of the detectors used in this analysis are listed in Table 1.

Neither the emitted α particle, nor the recoiling nucleus, carrying typically ≈120 keV, have mean free paths longer than a few

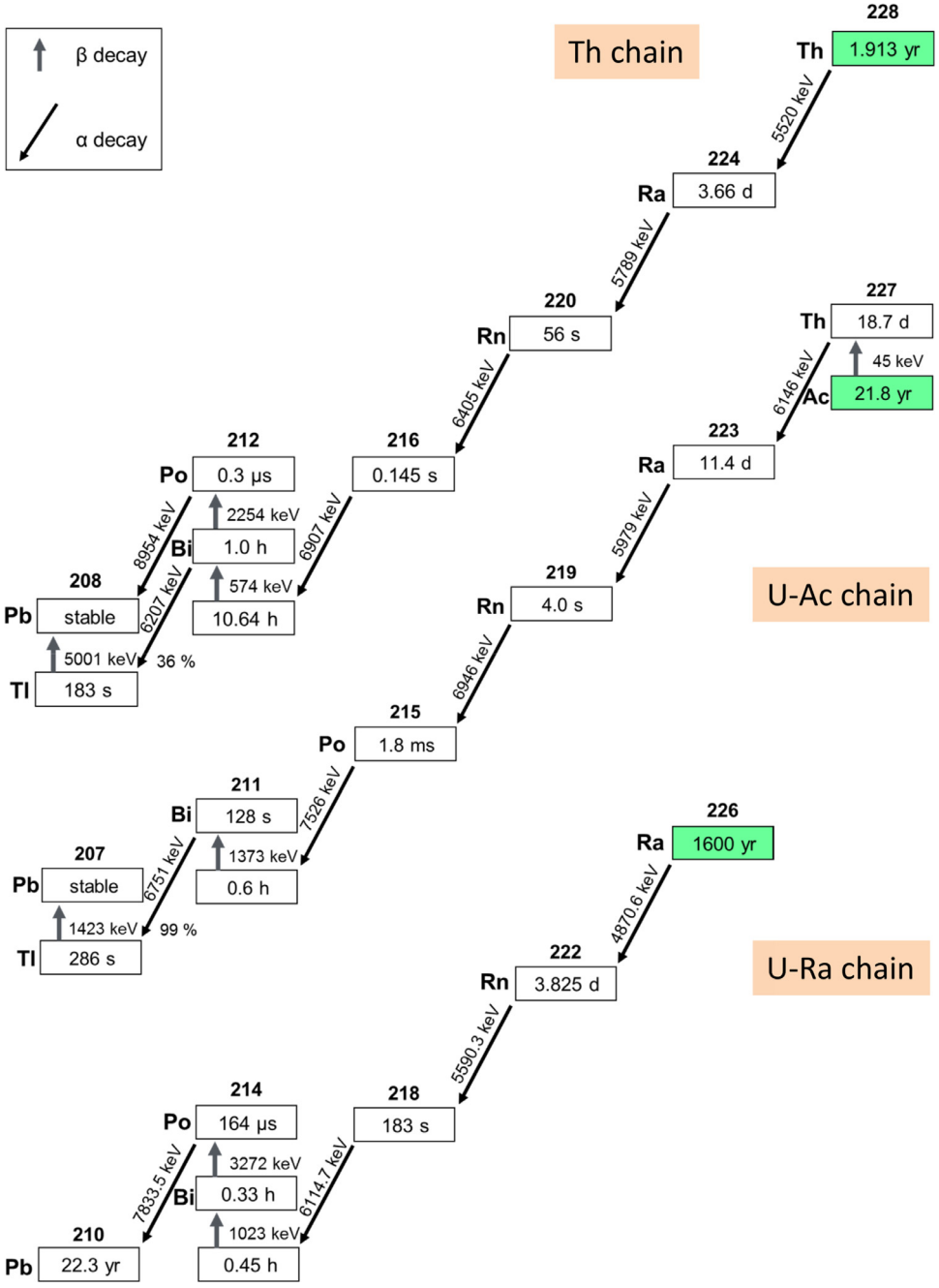

Fig. 1. Overview of the relevant isotopes in the three natural decay chains ^{232}Th (Th chain), ^{235}U (U-Ac chain) and ^{238}U (U-Ra chain). Energies, half-lives and branching ratios are given.

µm. Due to this reason only events with an energy deposited in a single detector, i.e. with multiplicity one, are selected without significant loss of exposure.

When a potential parent decay resulting from ^{228}Th, ^{227}Ac or ^{226}Ra or the subsequent daughter nuclei is found, the following time window of ten daughter half-lives is examined for the presence of a possible daughter decay. This search is performed for all α decays occuring in the sub-decay chains shown in Table 2. The probability for the daughter nucleus to decay within this time interval is higher than 99.9%. The energy intervals where this search is performed are:

$$E_{\max} = Q_\alpha + 100\,\mathrm{keV},$$
$$E_{\min} = E_{\alpha,\min} - 100\,\mathrm{keV}, \quad (1)$$

where Q_α is the Q-value of the decay and $E_{\alpha,\,\min}$ is the (lowest) energy of the α particle that populates the highest excited level of the daughter nuclei with branching ratios above 2.5%. Branching ratios below 2.5% have been disregarded leading to a reduction of efficiency of less than 4% for the ^{227}Ac sub-decay chain and less than 0.8% for the ^{226}Ra and ^{228}Th chains. The energy window is enlarged by ± 100 keV to account abundantly for the systematic uncertainty in energy calibration from possible preamplifier gain non-linearity for energies above 4.5 MeV [12]. While the uncertainty is estimated to be less than 50 keV at 6 MeV, it was decided to use the larger window size as it does not change the result thanks to the quasi background free analysis while being maximally conservative. By using the minimum α energy for determination of the lower bound on the energy window, also the uncer-

Table 1
Detector masses and live times. The active mass of GTF112 and GTF45 have been estimated from the average of those of the four ANG detectors.

detector	live time (days)	total mass (kg)	active mass (kg)
ANG2	543.8	2.833	2.468± 0.145
ANG3	543.8	2.391	2.070± 0.136
ANG4	543.8	2.372	2.136± 0.135
ANG5	543.8	2.746	2.281± 0.132
RG1	543.8	2.110	1.908± 0.125
RG2	411.8	2.166	1.800± 0.115
GD32B	282.4	0.717	0.638± 0.113
GD32C	305.9	0.743	0.677± 0.019
GD32D	286.3	0.723	0.667± 0.022
GD35B	305.9	0.812	0.742± 0.019
GTF32	154.7	2.321	2.251± 0.116
GTF45	154.7	2.312	2.242± 0.150
GTF112	543.8	2.965	2.571± 0.150

Table 2
Sub-decay chains considered in the search and corresponding energy windows where the search for α decay candidates is performed. The intervals are calculated according to Eq. (1) with values from [13]. The last column gives the averaged probability ϵ to observe the decay of the daughter nucleus (or the next α decay in the sequence in case the daughter nucleus is not an α emitting isotope) following the specific α decays listed for the detectors that have candidate events for all decays in the sub-decay chain.

chain	isotope	energy window (keV)	ϵ
U-Ra	^{226}Ra	4501–4971	1.000
	^{222}Rn	5389–5690	0.919
	^{218}Po	5902–6215	0.999
U-Ac	^{227}Th	5601–6246	1.000
	^{223}Ra	5440–6079	0.878
	^{219}Rn	6325–7046	1.000
	^{215}Po	7286–7626	1.000
	^{211}Bi	6178–6851	0.995
Th	^{228}Th	5240–5620	1.000
	^{224}Ra	5340–5889	0.921
	^{220}Rn	6188–6505	0.993
	^{216}Po	6678–7007	1.000

tainty on the quenching factor of the recoiling nucleus is taken into account, effectively allowing for a 100% ionization quenching of the recoil nucleus. The following analysis makes use only of part of the decay chains looking for α decays with branching ratios of $> 96\%$ as shown in Fig. 1 (see Table 2).

As the detection efficiency of α particles inside germanium detectors is basically 100%, from the non observa-tion of an intermediate decay within a chain it can be followed with high confidence that the mother nucleus of the observed decay can not have been inside the bulk of the material. The α decays and the corresponding energy windows to which the search is restricted are listed in Table 2.

The energy spectrum of all candidate α events without time coincidence cut for all detectors and for the complete data-taking period after selection based on Eq. (1) is shown in Fig. 2. The lowest energy of interest given in Table 2 is 4501 keV which defines the range in this figure. The gap in the spectrum appears due to the gap in the allowed energy ranges (see Table 2).

The contamination is calculated as the mass fraction C, i.e. the mass M of the isotope under consideration over the active mass of the detector $m_{\rm det}$:

$$C = \frac{M}{m_{\rm det}} = \frac{\nu\ m_A}{N_A\ m_{\rm det}(1-e^{-\lambda\Delta t})\,\epsilon} \simeq \frac{\nu\ m_A}{N_A\ \lambda\ \epsilon\ \mathcal{E}}\ , \qquad (2)$$

where N_A is Avogadro's number, ν is the number of detected events or the corresponding upper limit in case of no observed signal, m_A is the molar mass of the contaminating isotope, λ is the decay constant, $\mathcal{E} = m_{\rm det}\cdot\Delta t$ is the exposure. The last approximation in Eq. (2) can be used when the observation time is much shorter than the parent nuclide half-life (^{228}Th, ^{227}Ac and ^{226}Ra), which always holds true for this analysis. The efficiency, ϵ, accounts for detector dead times and the probability that subsequent events in a decay chain happen outside the active volume. It is estimated in Section 4 an given in Table 2.

3. Background estimation for time coincidence signature

The energy spectrum at the relevant energies for this analysis is dominated by α decays of ^{210}Po, ^{226}Ra, ^{222}Rn and ^{218}Po on the p+ surfaces of the detectors [12]. This surface contamination can be the source of successive decays that mimic the time and energy signature of signal α decays within the bulk. In the following we assume constant decay rates in the energy windows (see Table 2) taken from the α background model developed in Ref. [12]. In reality this is not accurate for the ^{210}Po part of the contamination. The analysis is, however, not sensitive to the details of the alpha background model. The probability density that a background event in the energy range expected for the daughter isotope $(i+1)$ will take place stochastically in time t after a background event i in the energy range corresponding to the mother isotope, is given by the product of the random time interval distribution of background events in the energy range of the daughter isotope $(i+1)$:

$$\frac{dp}{dt} = r_{i+1}\ e^{-r_{i+1}t}\ , \qquad (3)$$

where r_i is the mean background rate in the energy window of decay i. The integral of Eq. (3) from zero to $\Delta t_{i,i+1}$ is the probability to randomly observe the decay sequence $i, (i+1)$ within the time window $\Delta t_{i,i+1}$. The number of expected random coincidences from background events to the present chain analysis, i.e. random decay sequences that mimic the signal decay chain during the life time T is then given by:

$$n_b = r_1\ T \prod_{i=1}^{K-1}\left[1 - e^{-r_{i-1}\ \Delta t_{i,i+1}}\right]\ , \qquad (4)$$

where K is the number of decays in the sequence and $\Delta t_{i,i+1}$ are maximum time limits between two subsequent decays i and $(i+1)$, i.e. ten half-lives for the present analysis.

The α background model [12] was used to estimate the rates r_i in Eqs. (3) and (4). For a live time of 543.8 days, the number of stochastic coincidences, n_b, is $n_b < 5\cdot 10^{-15}$ for the ^{227}Th, $n_b < 1\cdot 10^{-13}$ for the ^{228}Th and $n_b < 0.94$ for the ^{226}Ra chain. The very low background expectations for the ^{227}Ac and ^{228}Th subchains appear due to the exponential suppression of the probability for stochastic coincidence with smallness of the time windows between two subsequent decays. Both sub-chains have two subsequent decays with time windows of the order of seconds or less.

An additional background component is due to ^{228}Th, ^{227}Ac or ^{226}Ra contamination on the p+ surfaces of the detectors. Such surface contaminations can lead to the same time signature while not being related to bulk contamination of the HPGe material itself. Considering a mother nucleus at rest on the p+ surface, the α particle and the daughter nucleus will have momenta in opposite directions. Hence, if the α particle is detected through energy deposition in the active volume, the daughter nucleus will likely recoil away from the p+ surface. In order to observe the decay of the daughter nucleus, its momentum needs to be pointing towards the active volume. However, in this case, the α particle from the preceeding decay of the mother nucleus will be traveling away from the active volume and likely remain undetected. Therefore, based on simple kinematic arguments, it is unlikely that all α decays from p+ surface contaminations will be observed. This argument

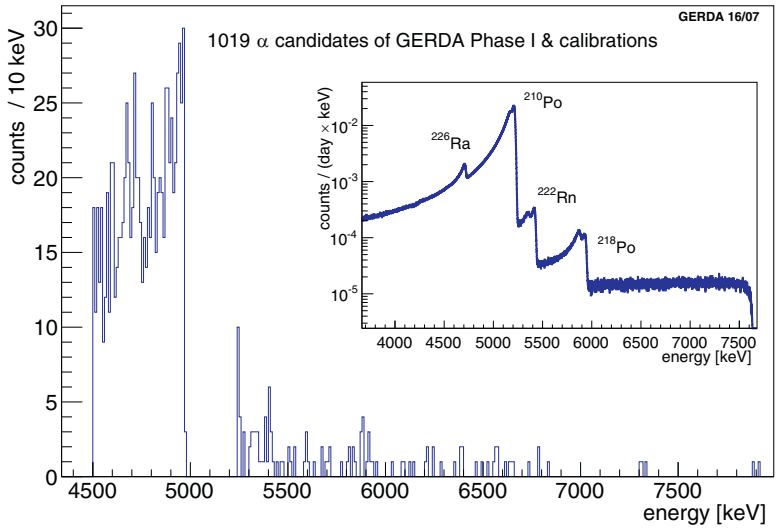

Fig. 2. Energy spectrum of α decay candidates from the uranium and thorium series for the whole data-taking period considered in this analysis. For comparison the inset shows the prediction by the background model for the sum of the enriched semi-coaxial detectors.

is supported by the observation that for the best fit background model in Phase I, the number of events from an initial ^{226}Ra contamination on the p+ surface is roughly halved for each subsequent decay [12]. In order to quantify this background for the ^{226}Ra sub-chain 10^5 decay chains originating from ^{226}Ra nuclei in the dead layer were simulated using MaGe [14]. From these simulations it is derived that the percentage of ^{226}Ra decays that will produce three subsequent α decays depositing energy in the active volume is expected to be 0.07%. For 50.5 ^{226}Ra decays on the p+ surface as derived from the α background analysis [12], the expected number of triple coincidences is less than 0.04.

4. Efficiency estimation

When nuclei of parent isotopes decay in the active volume of a detector, all subsequent decays of daughter nuclides in the related chain should be observable as long as the measuring time is considerably longer than the longest half-life in the chain. The probability that the daughter nucleus with typically ≈120 keV recoil energy after an α decay leaves the active volume of the detector due to its recoil is negligible, as the range of heavy ions with this recoil energy is only a few tens of nm. Hence, nuclei can be kicked out of the active volume only from the outer ≈50 nm of the detector, corresponding to an active volume fraction of $\approx 10^{-6}$ for detectors with ≈4 cm radius and ≈10 cm height.

For decays in the bulk of the detector without the emission of gamma particles the efficency of deposition of the full energy in the detector released in the decay is practically 100%. In this case the full energy released in the decay can be detected. Both the recoiling nucleus and the emitted α particle deposit their full energy with high probability in the active volume. For the recoiling nucleus the same argument holds as above. An α particle with a few MeV of kinetic energy has a stopping range of a few tens of µm [15]. Hence, the probability that it leaves the active volume will be larger, but still negligible with respect to the uncertainty on the active volume. Conservatively assuming that only α particles from the outer ≈50 µm shell of the active volume of the detector escape from the active volume, its fraction is reduced by approximately one permil.

If there are candidates for the decay of a mother nucleus of a given sub-decay chain, when searching for time correlations between two or more events, detector off times play a crucial role. As the subsequent decays could happen during detector off-time, the exposure has to be corrected. In order to conservatively estimate this change in effective exposure due to detector off-times, convolutions of the live time profile with the exponential decay probability density function (pdf) of the expected decay are used. In particular, for each 120 s time bin of each individual detector the exponential pdf of the subsequent α decays have been convoluted with the detector life time profiles following the given time bin. This provides the pdf of observing the daughter decay at that moment. The integral over this convoluted pdf then gives the reduction in effective life-time for the given bin. The average probabilities of observing the subsequent α decays within the decay chain are obtained by averaging over all time bins during the life time of the individual detectors. They are listed in the last column of Table 2. For detectors that have no candidate decay of the mother isotope or that have zero candidates of one of the isotopes of a sub-decay chain listed in Table 2 no change in effective exposure is taken into account.

The time averaged probability to observe all α decays in the chain after a candidate of the mother isotope has been detected, is 0.920 for ^{228}Th, 0.874 for ^{227}Ac and 0.918 for ^{226}Ra for the detectors in which there were candidate events for all decays in the sub-decay chain. These values are used to obtain the effective exposure $\epsilon \times \mathcal{E}$ in Eq. (2) for these detectors. Taking this loss in efficiency and all systematic uncertainties into account the effective exposure is reduced to 23.9 kg· yr for the ^{228}Th sub-decay chains, 24.1 kg· yr for the ^{227}Ac and 23.3 kg· yr for the ^{226}Ra.

5. Results

In total there are 1019 candidate α events. Table 3 shows the total number of α-candidate events in each individual detector during the whole corresponding life time for each individual decay considered. Most detectors have zero events for at least one step in the individual sub-decay chains. For these detectors it is evident without further analysis that no complete chain was observed within the life time.

Additionally a coincidence search was performed. No full decay chain could be identified.

In total the 1019 candidate α events produced 304 potential ^{226}Ra – ^{222}Rn, 65 ^{227}Th – ^{223}Ra, 42 ^{228}Th – ^{224}Ra, 1 ^{224}Ra – ^{220}Rn and 1 ^{222}Rn – ^{218}Po coincidences. These numbers can be compared with expectations from Eq. (2) using the background model: This simple estimation gives an expectation of ∼300 ^{226}Ra – ^{222}Rn, ∼50 ^{228}Th–^{224}Ra and ∼50 ^{227}Th–^{223}Ra stochastic coincidences. Additionally there is one potential triple coincidence for a part of the

Table 3
Number of candidate events in the individual detectors. Note that candidate events can appear for more than one decay due to overlap of the energy windows.

	ANG2	ANG3	ANG4	ANG5	RG1	RG2	GD32B	GD32C	GD32D	GD35B	GTF32	GTF45	GTF112
^{226}Ra	142	265	45	92	30	35	6	10	5	8	45	35	144
^{222}Rn	3	7	1	0	0	0	0	1	0	0	1	3	12
^{218}Po	1	2	3	0	1	0	0	0	0	0	2	0	6
^{227}Ac	5	7	5	1	1	0	0	0	0	1	3	2	14
^{223}Ra	7	7	4	1	0	0	0	1	0	1	2	2	17
^{219}Rn	2	3	3	2	0	0	1	0	0	0	0	5	5
^{215}Po	0	1	0	0	1	0	0	0	0	0	1	0	0
^{211}Bi	2	4	4	2	0	0	1	0	0	0	1	6	7
^{228}Th	10	14	2	7	1	0	0	2	0	0	2	4	20
^{224}Ra	9	13	3	2	0	0	0	1	0	0	2	3	21
^{220}Rn	1	1	3	2	0	0	0	0	0	0	1	2	3
^{216}Po	0	1	0	0	0	0	0	0	0	0	0	2	1

Table 4
Triple coincidence candidate for the Th chain in GTF112 starting with ^{228}Th.

candidate event	recorded energy (keV)	ΔE ($Q_\alpha - E$) (keV)	time	time to next event (days/half-lives)
^{228}Th	5400.5	119.5	Dec 12 20:54:41 2011	23.1 / 6.3
^{228}Th	5381.5	138.5	Dec 20 17:10:47 2011	15.3 / 4.2
^{224}Ra	5388.2	400.8	Jan 4 23:43:15 2012	0.0001/0.2
^{220}Rn	6283.2	121.8	Jan 4 23:43:26 2012	

^{228}Th sub-chain from ^{228}Th to ^{220}Rn. Note that the same event can be part of more than one candidate coincidence.

It is interesting to have a closer look at the triple coincidence in GTF112. Some information is detailed in Table 4. The isotope candidate, the recorded energy, the energy difference to Q_α and time of the event are listed in this table. The last column shows the time interval to the next candidate decay in the chain. There are two possible candidate events for the parent nucleus. It is worth noting that all candidate events have energies that differ from the Q-values of the corresponding decays by ≈120 keV. This is consistent with the expectation that only the energy from the α particle, and not the recoiling daughter nucleus, is detected as expected for surface events. In contrast, one should note that the energy deposit of the ^{224}Ra candidate in Table 4 is 300 keV less than the most probable energy of the emitted α particle being 5685.37 keV, with a probability of 94.92% [13]. The decay of ^{216}Po is missing.

A mono-parametric pulse shape analysis method to identify events on the p+ surface has been developed [16]. The discriminating parameter is the rise time between 5% and 50% of the maximum pulse amplitude, t_{5-50}. The events of Table 4 have a t_{5-50} of ≈110 ns. These values are below the cut threshold of 990 ns as given in Ref. [16] indicating that they are consistent with the expectation for surface events.

Having found no candidate for a full decay chain and conservatively assuming zero background, the 90% credibility interval (C.I.) Bayesian upper limit for the contamination is 2.3 events, considering all α decays in the chains from ^{227}Ac to ^{207}Pb and ^{228}Th to ^{212}Pb, respectively. In case of ^{226}Ra, the expected number of background events is 1 and the 90% C.I. limit is 2.3 events. Since the half-life of ^{227}Th is much smaller than the one for ^{227}Ac, secular equilibrium can be assumed, hence the limit on ^{227}Ac is given instead. The derived limits and activities, taking into consideration the effective exposures and uncertainties in the active mass of the detectors are shown in Table 5 in g/g and nBq/kg.

The 90% C.I. upper limit on the ^{226}Ra contamination is $8.6 \cdot 10^{-23}$ g/g. The limits on the concentration of ^{227}Ac and ^{228}Th are $1.1 \cdot 10^{-24}$ g/g and $1.0 \cdot 10^{-25}$ g/g, respectively. The upper 90% C.I. limit on the activity of ^{226}Ra is 3.1 nBq/kg, the limit on the activity of ^{227}Ac is 3.0 nBq/kg and the limit on the activity of ^{228}Th is 3.1 nBq/kg corresponding to a rate of less then 100 decays per year per ton of germanium.

Table 5
90% C.I. upper limits on the concentration of ^{226}Ra, ^{227}Ac and ^{228}Th bulk contamination in GERDA Phase I detectors, expressed in g/g are given in the middle column. The right column gives upper limits on the activities of the bulk contamination in GERDA Phase I detectors, expressed in nBq/kg.

	contamination [g/g]	activity [nBq/kg]
^{226}Ra	$8.6 \cdot 10^{-23}$	3.1
^{227}Ac	$1.1 \cdot 10^{-24}$	3.0
^{228}Th	$1.0 \cdot 10^{-25}$	3.1

It is a safe assumption, that in a purification process the ratio of the isotopes ^{228}Th and ^{232}Th stays constant. Since the production of the HdM and IGEX detectors about 2 decades have passed. Therefore any deviation from secular equilibrium of the ^{232}Th chain is strongly reduced by now [17] and from the limit of the ^{228}Th concentration we estimate the 90% C.I. upper limit of ∼4 nBq/kgfor ^{232}Th. Assuming secular equilibrium for the ^{238}U and ^{232}Th decay chains and a RoI window of 4 keV, the expected background index contributions are ≈0.05 and ≈0.01 cts/(RoI· ton· yr), respectively. This analysis shows that HPGe belongs among the most radiopure materials. With the same analysis with GERDA Phase II data with an exposure of 100 kg· yr we expect an improvement of the sensitivity to bulk alphas by a factor of roughly 5, i.e. a sub nBq/kg sensitivity.

6. Conclusions

A search for a possible presence of contamination, originating from the uranium and thorium natural radioactive decay chains, in the bulk of HPGe detectors in GERDA Phase I has been performed. No complete decay chain was observed. From the non-observation of full decay chains 90% C.L. upper limits were derived for the concentrations and activities of ^{228}Th, ^{227}Ac and ^{226}Ra in GERDA Phase I detectors. A contamination of detectors according to these limits would lead to a background index 0.1 cts/(RoI· ton· yr) in accordance with the requirements for a future ton scale double beta decay experiment based on germanium detectors.

Acknowledgments

The GERDA experiment is supported financially by the German Federal Ministry for Education and Research (BMBF), the German Research Foundation (DFG) via the Excellence Cluster Universe, the Italian Istituto Nazionale di Fisica Nucleare (INFN), the Max Planck Society (MPG), the Polish National Science Center (NCN), the Russian Foundation for Basic Research (RFBR), and the Swiss National Science Foundation (SNF). The institutions acknowledge also internal financial support.

References

[1] GERDA collaboration, K.-H. Ackermann, Eur. Phys. J. C 73 (2013) 2330.
[2] GERDA collaboration, M. Agostini, Phys. Rev. Lett. 111 (2013) 122503.
[3] M. Agostini, For the GERDA collaboration, on XXVII International Conference on Neutrino Physics and Astrophysics (Neutrino 2016), London 4.07.16-9.07.16, http://neutrino2016.iopconfs.org/IOP/media/uploaded/EVIOP/event_948/09.25__5__agostini.pdf.
[4] MAJORANA collaboration, N. Abgrall, Adv. High Energy Phys. 2014 (2014) 365432.
[5] K.H. Wedepohl, Geochimica et Cosmochimica Acta 59 (1995) 1217.
[6] K. Kröninger, Techniques to distinguish between electron and photon induced events using segmented germanium detectors, Technical University Munich, 2007 Phd thesis.
[7] H.V. Klapdor-Kleingrothaus, Eur. Phys. J. A 12 (2001) 147.
[8] C.E. Aalseth, Phys. Rev. D 65 (2002). 0920.
[9] L. Baudis, Astropart. Phys. 17 383 (2002).
[10] GERDA collaboration, M. Agostini, et al., Eur. Phys. J. C75 39 (2015).
[11] M. Agostini, L. Pandola, P. Zavarise, J. Phys. 368 (2012). 012047.
[12] GERDA collaboration, M. Agostini, Eur. Phys. J. C 74 (2014) 2764.
[13] S.Y.F. Chu, L.P. Ekström, R.B. Firestone. The Lund/LBNL Nuclear Data Search (1999).
[14] M. Boswell, et al., IEEE Trans. Nucl. Sci. 58 (2011) 1212.
[15] J.F. Ziegler, J.P. Biersack, M.D. Ziegler, SRIM, The Stopping and Range of Ions in Matter, SRIM Co., 2008.
[16] M. Agostini, Signal and background studies for the search of neutrinoless double beta decay in GERDA, Technical University Munich, 2013 Phd thesis.
[17] W. Maneschg, et al., Nucl. Inst. Meth. A 593 (2008) 448.